10

Spatially periodic hybrid structures based on opal films coated with a-Si:C:H layer: synthesis and emitting properties

© S.A. Grudinkin, N.A. Feoktistov, V.G. Golubev, S.I. Pavlov, A.A. Dukin, A.B. Pevtsov

Ioffe Institute, St. Petersburg, Russia

e-mail: grudink@gvg.ioffe.ru

Received May 23, 2025
Revised June 19, 2025
Accepted October 24, 2025

The luminescent response of a two-dimensional photonic crystal based on a hybrid structure formed from a synthetic opal film covered with an emitting layer of hydrogenated amorphous silicon-carbon alloy has been studied. Spectral-angular dependencies of photoluminescence intensity of the synthesized structure were recorded using spectral Fourier microscopy. In the spectral-angular dependencies of photoluminescence intensity in the visible wavelength range, characteristic peaks were observed, the appearance of which is associated with the interaction of radiation from a-Si:C:H nanoclusters with the radiating modes of the two-dimensional photonic crystal, characterized by a low group velocity.

Keywords: photonic crystal, Fourier transform spectral microscopy, photoluminescence, hydrogenated amorphous silicon-carbon alloy.

DOI: 10.61011/EOS.2025.10.62559.8015-25

Introduction

In recent years, active work has been underway to create new photonic structures that realize efficient resonant interaction of radiation with the active medium [1]. Two-dimensional ($2D$) photonic crystals (PCs) are considered among the most promising dielectric media for achieving light amplification due to an increase in the probability of radiative recombination, described by the Purcell factor [2]. Among various approaches proposed to increase luminescence signal intensity, one of the most promising is based on the interaction of radiative modes of PCs with low group velocity and luminescent centers whose emission lies energetically inside the light cone above the photonic bandgap of the $2D$ PC [3]. Such interaction does not require the formation of a microcavity, which significantly simplifies the fabrication of such structures. For example, [2] reports data on increased PL intensity in the spectral range of $800-1100$ nm in a silicon $2D$ PC with a triangular lattice of air holes. Publications [4,5] demonstrate increased PL intensity in $2D$ PCs formed on the basis of silicon structures with self-assembling Ge(Si) nanoislands.

In this work, spectral-angular dependences of the photoluminescence (PL) response intensity of hybrid structures formed from synthetic opal films coated with a luminescent layer of hydrogenated amorphous silicon-carbon alloy (a-Si:C:H) were investigated. The a-Si:C:H layer and the underlying top monolayer of hexagonally close-packed spherical amorphous silica (a-SiO_2) particles form an $2D$ photonic crystal structure. In this structure, the a-Si:C:H, layer serves as the emitter, exhibiting intense PL in the visible wavelength range. The spectral position of the PL contour can be easily varied by changing the carbon content in the a-Si:C:H film. The full width at half maximum (FWHM) of the a-Si:C:H PL contour reaches $0.6-0.7$ eV. The high FWHM value can be explained by the fact that carbon-enriched films represent a heterogeneous fine-grained system in which individual nanogranules are isolated from each other by high potential barriers [6].

Experimental Method

Opal films from close-packed monolayers of a-SiO_2 spherical particles with a diameter of ~ 520 nm were grown by liquid-phase colloidal epitaxy on a fused quartz substrate [7]. The particle size dispersion by diameter was $\sim 5\%$. Growth layers parallel to the substrate surface corresponded to the (111) crystallographic plane. The opal films were then coated with an a-$Si_{1-x}C_x$:H layer by plasma-enhanced chemical vapor deposition using a silane-methane-argon gas mixture. The ratio of gas flows of carbon- and silicon-containing components in the gas mixture corresponded to the film composition with $x = 0.58$ [8]. The a-Si:C:H layers were deposited simultaneously on the opal film and an adjacent quartz substrate (reference sample) in a single technological cycle and had nearly identical thickness ~ 240 nm. The PL band maximum of a-Si:C:H was at a wavelength of ~ 700 nm, with FWHM of ~ 200 nm. The refractive index of the a-Si:C:H film was determined using spectral ellipsometry [8].

Spectral-angular PL intensities of the synthesized $2D$ PCs were studied using spectral Fourier microscopy [9]. For PL excitation, a 405 nm laser diode was used, with its radiation focused onto the sample from the substrate side using an Olympus $20\times$ objective with numerical aperture $N_A = 0.4$. PL signal detection was performed using an

Olympus Plan FL 100× objective with numerical aperture $N_A = 0.95$. Unpolarized PL signal was measured in the wavelength range 400−1100 nm and emission angle range relative to the surface normal 0−50° using an Acton SP2500i spectrometer with a 300 mm^{-1} diffraction grating and CCD matrix (Princeton Instruments PIXIS 256) as the detector. The CCD matrix had 256 × 1024 pixels. The spectral resolution of the setup was 0.2 nm, and the angular resolution ∼ 0.2°.

Calculation procedure

Optical response spectra of spatially periodic hybrid structures and the PC band diagram were calculated using the modal Fourier method in the form of a scattering matrix (rigorous coupled wave analysis — RCWA) [10]. In this method, solutions to Maxwell's equations for each layer are found by expanding the electric and magnetic fields into Floquet-Fourier modes (plane waves). The exact solution can be represented as an infinite series over these modes. In the calculations, special attention was paid to selecting an adequate shape for the *a*-Si:C:H cover layer. It was found that the „semicrescent" model (Fig. 1, *c*) best describes the influence of the cover layer on the optical properties of the studied structures [11]. The refractive index of opal spheres was determined from analysis of Bragg reflection spectra of the original opal film and taken as 1.92.

For calculating the radiative ability spectra of the *a*-Si:C:H layer, a method based on the electrodynamic reciprocity principle was used, according to which the problem reduces to calculating the electric near field of a plane wave in the emitting layer. With this approach, the problem of calculating radiation from randomly distributed and randomly polarized oscillating dipoles is replaced by a problem in which the structure is illuminated by a polarized plane wave $E_{\text{in}}(x, y, z) = E_x(y)\exp(ik_0 z - i\omega t)$. The resulting electric field distribution in the *a*-Si:C:H layer, $I_j = \iint dxdy(|E_{jx}|^2|E_{jy}|^2)$ then gives the corresponding polarized component of the emission intensity [12].

Results and Discussion

Fig. 1, *a* shows an atomic force microscopy (AFM) image of the *a*-Si:C:H/opal hybrid structure surface. The *a*-Si:C:H film uniformly covers the *a*-SiO_2 spherical particles forming a closely-packed layer perpendicular to the opal film growth direction [111]. The inset to Fig. 1, *a* shows a defective area of the hybrid structure where the *a*-Si:C:H film is partially absent, revealing the surface of the *a*-SiO_2 spheres. AFM relief measurement in the defective area allowed determination of the *a*-Si:C:H film thickness which is equal to ∼ 240 nm.

The diffraction pattern of monochromatic light (405 nm) at normal incidence of the laser beam on the sample from the substrate side is shown in Fig. 1, *b*. Due to the two-dimensional spatial periodicity of the structure, the

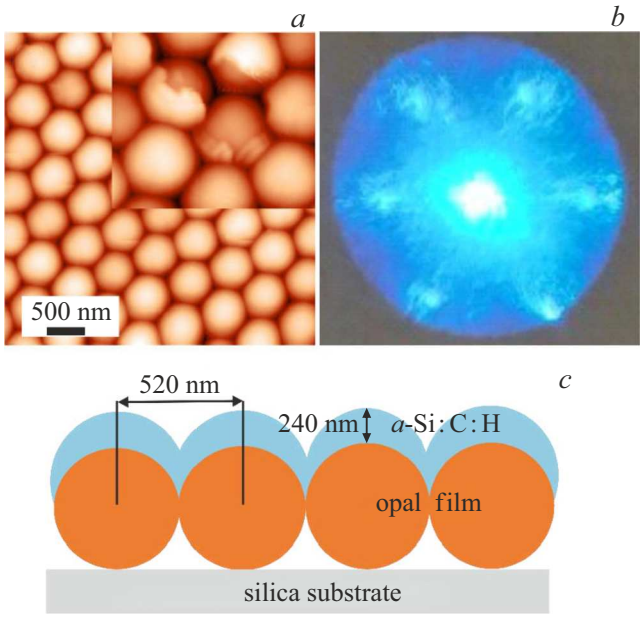

Figure 1. AFM image of the 2*D* PC *a*-Si:C:H/opal (*a*). The inset shows a fragment of the structure where the *a*-Si:C:H film is partially absent, revealing *a*-SiO_2 spheres. Diffraction pattern of monochromatic light (405 nm) on the *a*-Si:C:H/opal hybrid structure (*b*). Schematic view of the hybrid structure used in calculations. For simplicity, only one monolayer of *a*-SiO_2 spheres is shown (*c*).

diffraction pattern in this observation geometry consists of six reflexes characterized by C_6 symmetry relative to the incident beam. In the experiment, the structure was oriented such that two of the six reflexes lay in the horizontal plane. The PL signal detection plane passed through one of the three equivalent pairs of nodes of the hexagonal reciprocal lattice: (-11) (1-1); (01) (0-1); (-10) (10). In modeling, we assumed that the vertical section of the *a*-Si:C:H layer has a semicrescent shape. A schematic image of the structure section is shown in Fig. 1, *c*.

Experimental spectral-angular dependences of PL intensity for the synthesized hybrid structure are presented in Fig. 2, *a* and *b*. Thanks to the broad *a*-Si:C:H PL contour, a large number of peaks can be simultaneously observed in the experimental PL spectra in the wavelength range 550−900 nm with their spectral positions depending on the emission angle. At angles close to zero, the PL spectrum features the most intense peak at 735 nm with a broad short-wavelength wing (Fig. 2, *b*). With increasing emission angle, the position of the most intense peak experiences a long-wavelength shift, and at 8° this peak acquires a doublet structure due to the appearance of a short-wavelength peak at 700 nm. With further angle increase, the doublet shifts toward shorter wavelengths. Note that, according to Bragg reflection spectra, the 3*D* photonic stop-band for the opal films studied in this work, formed from *a*-SiO_2 spheres with a diameter of ∼ 520 nm is located in the near-IR spectral

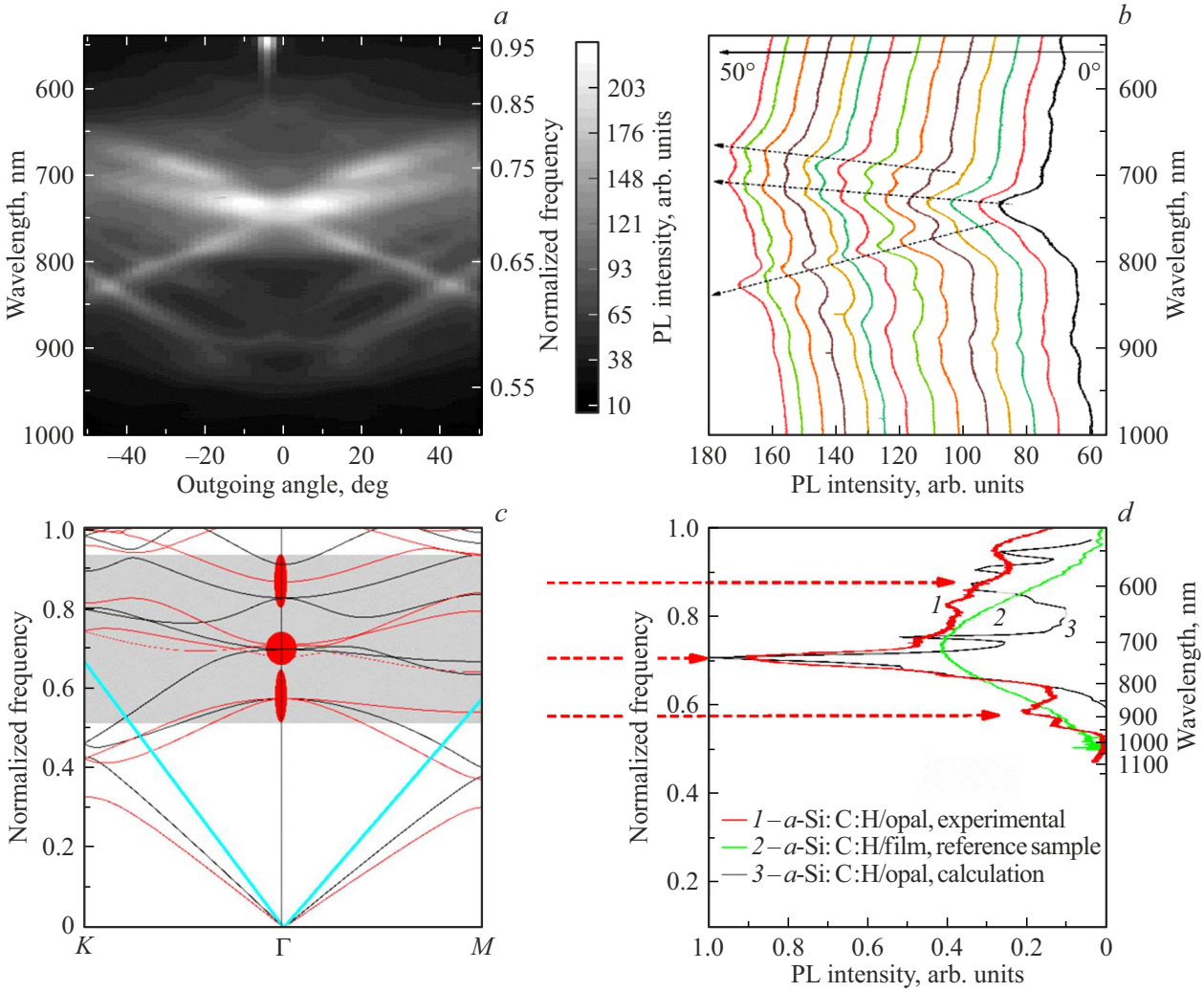

Figure 2. Photoluminescence (PL) spectra and band diagram of the *a*-Si:C:H/opal–two-dimensional photonic crystal: experimental spectral-angular dependences of PL intensity measured by spectral Fourier microscopy (*a*); PL spectra recast in (wavelength/intensity) coordinates for detection angles in the range 0–50°, graphs shifted along the ordinate axis for comparison convenience (*b*); band diagram of 2*D* PC *a*-Si:C:H: own PC modes are shown (red lines — TM modes, black — TE modes) and light cone (slanted straight blue lines), gray rectangle corresponds to the spectral PL range for the *a*-Si:C:H sample, regions with near-zero group velocity near the Γ- point of the Brillouin zone and corresponding PL spectrum peaks are marked with red ellipses and dashed arrows (*c*); experimental PL spectra at zero emission angle of 2*D* PC *a*-Si:C:H/opal (*1*), PL spectrum of the reference *a*-Si:C:H film (*2*), PL spectrum calculated using the modal Fourier method in scattering matrix form (*3*) (*d*).

region (1100–1200 nm) and does not affect the spectra measured in the visible range.

Fig. 2, *c* shows the calculated band diagram of the 2*D* PC. It can be seen that in the spectral region corresponding to the *a*-Si:C:H PL contour (gray band), there are numerous dispersion curves with complex $\omega(\kappa)$ dependence. The emission of *a*-Si:C:H nanoclusters overlaps with several radiative modes localized in the vicinity of the Γ-point in the Brillouin zone of the 2*D* PC which are located inside the light cone and, as calculations show, are characterized by low group velocity $d\omega/d\kappa \approx 0$. The interaction of *a*-Si:C:H nanocluster emission with PC modes causes the strong transformation of the PL spectrum observed experimentally. A detailed analysis of the connection between the observed spectral-angular PL dependences and the calculated band diagram will be presented in a separate publication.

Here we consider in more detail only the PL spectra at zero emission angle. Fig. 2, *d* shows the experimental PL signal dependences for the 2*D* PC *a*-Si:C:H/opal and the reference *a*-Si:C:H film deposited on a fused quartz substrate, measured at an emission angle close to 0 (i.e., near the Γ point of the Brillouin zone). It is evident that interaction with PC radiative modes having near-zero group velocity (marked by red ellipses on the energy band diagram, Fig. 2, *c*), leads to substantial spectrum narrowing and an ~ 2.5 increase in peak PL intensity compared to the

reference sample. The figure also shows the PL spectrum for the studied hybrid structure calculated using the modal Fourier method in scattering matrix form. Comparison of the spectra shows good agreement between theory and experiment (see arrows in Fig. 2, *d*). The discrepancy may be due to the simplified nature of the calculation, which does not account for the influence of the lower layers of the 10-layer opal film.

Conclusion

This work presents results of studying the luminescent response of an 2*D* PC based on a spatially periodic hybrid structure opal film coated with an emitting α-Si:C:H layer using spectral Fourier microscopy. In the 500−1000 nm wavelength range, characteristic peaks with various angular dependences were found in the 2*D* PC PL spectra. Comparison of experimental PL spectra with the calculated 2*D* PC energy band diagram allows the conclusion that the peaks observed experimentally in the spectral-angular PL dependence of the hybrid structure arise due to the interaction of *a*-Si:C:H nanocluster emission with PC radiative modes located inside the light cone and characterized by low group velocity. The hybrid structures obtained in this work are of interest both for fundamental studies of radiation interaction with active media and for practical applications in selective enhancement of luminescent response.

Funding

The work was performed under state assignment No FFUG-2024-0017.

Conflict of interest

The authors declare that they have no conflict of interest.

References

[1] Z. Qian, L. Shan, X. Zhang, Q. Liu, Y. Ma, Q. Gong, Y. Gu. Photonics, **2**, 1 (2021). DOI: 10.1186/s43074-021-00043-z
[2] A. Mahdavi, G. Sarau, J. Xavier, T.K. Paraïso, S. Christiansen, F. Vollmer. Scientific Reports, **6** (1), 25135 (2016). DOI: 10.1038/srep25135
[3] A.I. Kuznetsov, M.L. Brongersma, J. Yao, M. K. Chen, U. Levy, D.P. Tsai, N.I. Zheludev, A. Faraon, A. Arbabi, N. Yu, D. Chanda, K.B. Crozier, A.V. Kildishev, H. Wang, J.K.W. Yang, J.G. Valentine, P. Genevet, J.A. Fan, O.D. Miller, A. Majumdar, J.E. Fröch, D. Brady, F. Heide, A. Veeraraghavan, N. Engheta, A. Alu, A. Polman, H.A. Atwater, P. Thureja, R. Paniagua-Dominguez, S.T. Ha, A.I. Barreda, J.A. Schuller, I. Staude, G. Grinblat, Y. Kivshar, S. Peana, S.F. Yelin, A. Senichev, V.M. Shalaev, S. Saha, A. Boltasseva, J. Rho, D.K. Oh, J. Kim, J. Park, R. Devlin, R.A. Pala. ACS Photonics, **11** (3), 816 (2024). DOI: 10.1021/acsphotonics.3c00457
[4] D.V. Yurasov, A.V. Novikov, S.A. D'yakov, M.V. Stepihova, A.N. Yablonskij, S.M. Sergeev, D.E. Utkin, Z.F. Krasil'nik. FTP, **54** (8), 822 (2020) (in Russian). DOI: 10.21883/FTP.2020.08.49633.10
[5] A.V. Peretokin, D.V. Yurasov, M.V. Stepikhova, M.V. Shaleev, A.N. Yablonskiy, D.V. Shengurov, S.A. Dyakov, E.E. Rodyakina, Z.V. Smagina, A.V. Novikov. Nanomaterials, **13** (1), 1678 (2023). DOI: 0.3390/nano13101678
[6] V.A. Vasil'ev, A.S. Volkov, E. Musabekov, E.I. Terukov, V.E. Chelnokov, S.V. Chernyshev, Yu.M. Shernyakov. FTP, **24** (4), 710 (1990) (in Russian).
[7] P. Jiang, J. Bertone, K.S. Hwang, V. Colvin. Chem. Mater., **11** (8), 2132 (1999). DOI: 10.1021/cm990080+
[8] M.V. Rybin, A.V. Zherzdev, N.A. Feoktistov, A.B. Pevtsov. Phys. Rev. B, **95** (16), 165118 (2017). DOI: 10.1103/PhysRevB.95.165118
[9] R. Wagner, L. Heerklotz, N. Kortenbruck, F. Cichos. Appl. Phys. Lett., **101** (8), 081904 (2012). DOI: 10.1063/1.4746251
[10] S.G. Tikhodeev, A. Yablonskii, E. Muljarov, N.A. Gippius, T. Ishihara. Phys. Rev. B, **66** (4), 045102 (2002). DOI: 10.1103/PhysRevB.66.045102
[11] S. Dyakov, N. Gippius, M. Voronov, S. Yakovlev, A. Pevtsov, I. Akimov, S. Tikhodeev. Phys. Rev. B, **96**, 045426 (2017). DOI: 10.1103/PhysRevB.96.045426
[12] S.A. Dyakov, D.M. Zhigunov, A. Marinins, M.R. Shcherbakov, A.A. Fedyanin, A.S. Vorontsov, P.K. Kashkarov, S. Popov, M. Qiu, M. Zacharias, S.G. Tikhodeev, N.A. Gippius. Phys. Rev. B, **93** (20), 205413 (2016). DOI: 10.1103/PhysRevB.93.205413

Translated by J.Savelyeva